Title

Negative Stefan-Maxwell diffusion coefficients and complete electrochemical transport characterization of homopolymer and block copolymer electrolytes

Journal

Journal of the Electrochemical Society, 165(11)

ISSN

0013-4651

Authors

Villaluenga, I
Pesko, DM
Timachova, K
et al.

Publication Date

2018

DOI

10.1149/2.0641811jes

Negative Stefan-Maxwell Diffusion Coefficients and Complete Electrochemical Transport Characterization of Homopolymer and Block Copolymer Electrolytes

Irune Villaluenga,[1,2,3,=] Danielle M. Pesko,[1,2,=] Ksenia Timachova,[1,2] Zhange Feng,[4] John Newman,[1,5,*] Venkat Srinivasan,[3,4,] and Nitash P. Balsara[1,2,3,5,**,z]**

[1]Department of Chemical and Biomolecular Engineering, University of California, Berkeley, California 94720, USA
[2]Materials Science Division, Lawrence Berkeley National Laboratory, Berkeley, California 94720, USA
[3]Joint Center for Energy Storage Research (JCESR), Lawrence Berkeley National Laboratory, Berkeley, California 94720, USA
[4]Argonne National Laboratory, Lemont, Illinois 60439, USA
[5]Energy Technologies Area, Lawrence Berkeley National Laboratory, Berkeley, California 94720, USA

Nanostructured block copolymers are of particular interest as electrolytes in batteries with lithium metal anodes. The performance of electrolytes in batteries can be predicted only if three transport coefficients (ionic conductivity, κ, salt diffusion coefficient, D, and cation transference number, t_+^0) are known. We present complete electrochemical transport characterization of a microphase-separated SEO block copolymer electrolyte by reporting κ, D, and t_+^0 as functions of salt concentration. We compare the properties of the block copolymer electrolyte with those of PEO homopolymer electrolytes. Negative values of t_+^0 are observed in many cases. Recasting the transport parameters in terms of Stefan-Maxwell coefficients provides insight into the nature of ion transport in these electrolytes.
 [DOI: 10.1149/2.0641811jes]

Manuscript submitted May 23, 2018; revised manuscript received August 10, 2018. Published August 25, 2018.

There is continuing interest in developing polymer electrolytes for lithium batteries.[1–3] Block copolymer electrolytes with a rigid nonconducting block and a soft conducting block are of particular interest as they enable decoupling of electrochemical and mechanical properties.[4,5] The performance of electrolytes in batteries can be predicted using concentrated solution theory only if three transport coefficients are known. In many studies,[6–11] the transport coefficients used are ionic conductivity, κ, salt diffusion coefficient, D, and cation transference number, t_+^0. While the second law of thermodynamics requires κ and D to be positive, t_+^0 can be positive or negative. We note in passing that most of the literature on polymer electrolytes is restricted to measurement and interpretation of ionic conductivity. In recent years, two approximate methods for measuring the transference number have gained in popularity: the steady-state current method[12,13] and the NMR method.[14–17] The relationship between the approximate transference numbers determined by these methods and t_+^0 is complex.[18–21]

In concentrated solution theory developed by Newman,[22] the transport of ionic species is governed by Stefan-Maxwell diffusion coefficients, $\mathfrak{D}_{+0}$, $\mathfrak{D}_{-0}$, and $\mathfrak{D}_{+-}$. These coefficients quantify the relationship between the gradient of electrochemical potential ($\nabla\mu_i$) and velocity of species ($\mathbf{v}_i$) obtained under this gradient:

$$c_i \nabla\mu_i = RT \sum_j \frac{c_i c_j}{c_T \mathfrak{D}_{ij}} \left(\mathbf{v}_j - \mathbf{v}_i\right),\ i, j = +,\ -,\ 0, \qquad [1]$$

where the subscripts refer to the cation, anion, and solvent, c_i are the molar concentration of species i, and c_T is the total molar concentration of the solution. In high-molecular-weight polymer electrolytes, the "solvent" is essentially immobile ($\mathbf{v}_0 = 0$). We are thus mainly interested in the relationships between $\nabla\mu_+$ and $\nabla\mu_-$ and $\mathbf{v}_+$ and $\mathbf{v}_-$.

In concentrated solution of a salt $(M^{z+})_{\nu_+}(X^{z-})_{\nu_-}$, the transference number is related to Stefan-Maxwell diffusion coefficients,

$$t_+^0 = \frac{z_+\mathfrak{D}_{+,0}}{z_+\mathfrak{D}_{+,0} + z_-\mathfrak{D}_{-,0}}. \qquad [2]$$

For the case of a univalent salt, Equation 2 reduces to

$$t_+^0 = \frac{\mathfrak{D}_{+,0}}{\mathfrak{D}_{+,0} + \mathfrak{D}_{-,0}}. \qquad [3]$$

In the simplest case $\mathfrak{D}_{+,0}$ and $\mathfrak{D}_{-,0}$ are positive, and t_+^0 is bounded between 0 and 1. If on the other hand t_+^0 is negative, as reported in Refs. 18 and 20, then one or more Stefan-Maxwell diffusion coefficients must be negative. This implies that the salt does not dissociate into individual cation and anion; instead charged clusters are obtained. For example, a negative $\mathfrak{D}_{-,0}$ implies that the net velocity of the anion due to electric migration alone is toward the negative electrode (i.e., the direction of $\mathbf{v}_-$ is opposite to that of $\nabla\mu_-$, see Equation 1). This is expected if the anion is clustered with two cations, and this cluster is fairly mobile. Direct evidence for the presence of such clusters can be obtained by electrophoretic nuclear magnetic resonance experiments (e-NMR).[15,23] Since the signs of Stefan-Maxwell diffusion coefficients are not constrained to be positive, many combinations of $\mathfrak{D}_{+,0}$ and $\mathfrak{D}_{-,0}$ can, in principle, lead to the observed negative transference numbers. For example, $\mathfrak{D}_{+,0} = -1$ (units are unimportant as we are mainly interested in ratios of $\mathfrak{D}_{ij}$) and $\mathfrak{D}_{-,0} = +2$ gives $t_+^0 = -1$. However, $\mathfrak{D}_{+,0} = +1$ and $\mathfrak{D}_{-,0} = -2$ also gives $t_+^0 = -1$. We show that one of these combinations violates thermodynamics. The advantage of determining Stefan-Maxwell diffusion coefficients (as opposed to the equivalent determination of κ, D, and t_+^0) is that they provide insight into the magnitude and direction of ion migration.

In this paper, we present complete electrochemical characterization of a high-molecular-weight nanostructured polystyrene-*b*-poly(ethylene oxide) (SEO) copolymer electrolyte doped with a lithium salt. Measurements of κ, D, and t_+^0 are used to determine Stefan-Maxwell diffusion coefficients. In several cases, we find that the diffusion coefficients are negative. Implications of these measurements on ion migration are discussed. For completeness, we compare results obtained from block copolymer electrolyte with those obtained from mixtures of poly(ethylene oxide) (PEO) homopolymer doped with lithium salt over the same concentration window.

Experimental

Materials.—Anhydrous tetrahydrofuran (THF) and benzene were purchased from Sigma-Aldrich, poly(ethylene oxide) (PEO, M_w = 5 kg/mol) with –OH endgroups was purchased from Polymer Source,

[=]These authors contributed equally to this work.
[*]Electrochemical Society Fellow.
[**]Electrochemical Society Member.
[z]E-mail: nbalsara@berkeley.edu

Table I. Values of *r, ρ, c, c_0,* and *m* for PEO homopolymer electrolytes.

r	ρ (g/L)	*c* (mol/L)	c_0 (mol/L)	*m* (mol/kg)
0.01	1160	0.25	24.72	0.23
0.02	1180	0.47	23.70	0.45
0.04	1210	0.87	21.79	0.91
0.06	1230	1.20	20.07	1.36
0.08	1330	1.59	19.85	1.82
0.10	1365	1.88	18.76	2.27
0.12	1380	2.11	17.58	2.73
0.14	1430	2.38	16.98	3.18
0.16	1450	2.58	16.11	3.64
0.18	1470	2.76	15.36	4.09
0.21	1516	3.05	14.53	4.77
0.24	1580	3.36	13.99	5.45
0.27	1572	3.49	12.93	6.14
0.30	1640	3.78	12.60	6.82

and lithium bis(trifluoromethanesulfone)-imide, $Li[N(SO_2CF_3)_2]$ (LiTFSI), was purchased from Novolyte. The chemicals were used as received. The polystyrene-block-poly(ethylene oxide) copolymer (PS: 240 kg/mol and PEO: 260 kg/mol, SEO) was synthesized by sequential anionic polymerization of styrene followed by ethylene oxide using methods described previously.[4]

Electrolyte preparation.—PEO electrolytes were prepared according to the procedures outlined in Ref. 18. All electrolytes are homogeneous mixtures of PEO and LiTFSI. Electrolytes are prepared at varying salt concentrations, ranging from $m = 0.23$ to $m = 6.82$ mol/kg, where *m* is the molality of the conducting phase.

Block copolymer electrolytes (SEO) were prepared by mixing SEO block copolymer and LiTFSI in dry DMF using a hot plate at 110°C for 12 h to obtain homogeneous solutions at different salt concentrations (from $m = 0.45$ to $m = 6.82$ mol/kg).

The characteristics of these electrolytes – density of the conducting phase, volume fraction of the conducting phase, ϕ_c, salt concentration, *c*, conducting phase concentration, c_0, and the molality of the conducting phase, *m* – are summarized in Table I for PEO electrolytes and Table II for SEO electrolytes. The volume fraction of the conducting phase in SEO electrolytes, ϕ_c, was calculated according to the equation used in Ref. 24. Salt concentration, *c*, was calculated according to

$$c = \frac{\rho r}{M_{EO} + r M_{LiTFSI}}, \qquad [4]$$

where ρ is the density of the PEO conducting phase, *r* is the molar ratio of lithium atoms to ethylene oxide (EO) moieties, M_{EO} and M_{LiTFSI} are the molar masses of ethylene oxide unit (44.05 g mol^{-1}), and LiTFSI (287.08 g mol^{-1}). Conducting-phase concentration, c_0, was calculated

Table II. Values of *r*, ρ, ϕ_c, *c*, c_0 and *m* for SEO block copolymer electrolytes. These values reflect calculated salt concentrations in the PEO microphase of SEO block copolymer.

r	ρ (g/L)	ϕ_c	*c* (mol/L)	c_0 (mol/L)	*m* (mol/kg)
0.02	1180	0.51	0.47	23.70	0.45
0.035	1229	0.52	0.80	22.72	0.80
0.05	1266	0.53	1.08	21.68	1.14
0.085	1340	0.55	1.66	19.57	1.93
0.10	1365	0.56	1.88	18.76	2.27
0.12	1380	0.57	2.11	17.58	2.73
0.15	1444	0.59	2.49	16.58	3.41
0.20	1505	0.61	2.97	14.83	4.55
0.25	1554	0.64	3.36	13.42	5.68
0.30	1640	0.65	3.78	12.60	6.82

according to

$$c_0 = \frac{c}{r}. \qquad [5]$$

The molality of the electrolyte, *m*, is calculated according to

$$m = \frac{r}{M_{EO}}. \qquad [6]$$

Electrochemical characterization.—All sample preparation steps were performed inside an argon glove box (MBraun) in order to maintain water and oxygen levels below 1 and 5 ppm, respectively. PEO electrolytes for conductivity, steady-state current, restricted-diffusion measurements, and concentration-cell experiments were prepared according to the procedures outlined in Ref. 18. SEO electrolytes for conductivity measurements were prepared by heat-pressing the polymer at 90°C into a 150 μm thick fiberglass−epoxy annular spacer (Garolite-10). The diameter of the electrolyte was taken to be the size of the hole in the annulus, 3.175 mm. High-purity aluminum foils, 17.5 μm thick, were pressed onto either side of the polymer as electrodes, and aluminum tabs (MTI corporation) were attached to the electrodes with polyimide tape. The sample assembly was vacuum-sealed in an airtight aluminum-reinforced polypropylene pouch with tabs protruding out so the sample could be electrically probed. The thickness of the polymer sample was measured after conductivity measurements were performed using a precision micrometer. Impedance spectroscopy measurements were performed using a VMP3 potentiostat (Bio-Logic) with an ac amplitude of 20 mV in the frequency range 1 MHz to 1 Hz. The ionic conductivity of the conducting phase in polymer electrolytes, κ, is calculated from the measured sample thickness, *L*, the cross-sectional area of the spacer, *S*, and bulk resistance, $R_{b,0}$, which was determined by methods discussed in the literature.[25] The conductivity is given by: $\kappa\ (T) = L/(S * R_{b,0}\ (T))$.

Lithium symmetric cells were prepared for steady-state current and restricted-diffusion measurements of SEO electrolytes. Samples were made by pressing the polymer electrolyte into a Garolite-10 spacer at 90°C for 10 s. After that, the electrolytes were sandwiched between two 150 μm lithium metal chips. Nickel tabs were secured to the lithium chips to serve as electrical contacts. The assembly was vacuum sealed in a laminated aluminum pouch material (Showa-Denko) before removal from the glove box. All samples were annealed at 90°C for 2 h prior to electrochemical characterization.

Steady-state current and restricted-diffusion measurements of SEO electrolytes were performed using a Biologic VMP3 potentiostat. All measurements were performed at 90°C. At the beginning of the experiment, cells were conditioned for 3 charge/discharge cycles at a low current density of 0.06 mA/cm^2. Each conditioning cycle consisted of a 4 h charge followed by a 4 h rest and a 4 h discharge. ac impedance spectroscopy was performed prior to potentiostat polarization. Complex impedance measurements were acquired for a frequency range of 1 MHz to 1 Hz at an amplitude of 40 mV. The cell resistances were measured as a function of time by performing ac impedance spectroscopy every 10 min during polarization. Here, the center of the ac input signal was offset by ΔV, and the amplitude was set to 20 mV to minimize disturbance of the polarization signal.

The transference number was determined according to

$$t_{+,SS} = \frac{i_{SS}\left(\Delta V - i_\Omega R_{i,0}\right)}{i_\Omega\left(\Delta V - i_{SS} R_{i,SS}\right)}, \qquad [7]$$

where ΔV is the applied potential, i_{SS} is the current measured at steady-state, and $R_{i,0}$ and $R_{i,SS}$ are the initial and steady-state resistances of the interface, respectively. This is the Bruce-Vincent-Watanabe approach for approximately measuring the transference number of electrolytes, and it is only valid for ideal solutions.[12,13] i_Ω is the initial current calculated according to this equation

$$i_\Omega = \frac{\Delta V}{R_{i,0} + R_{b,0}}, \qquad [8]$$

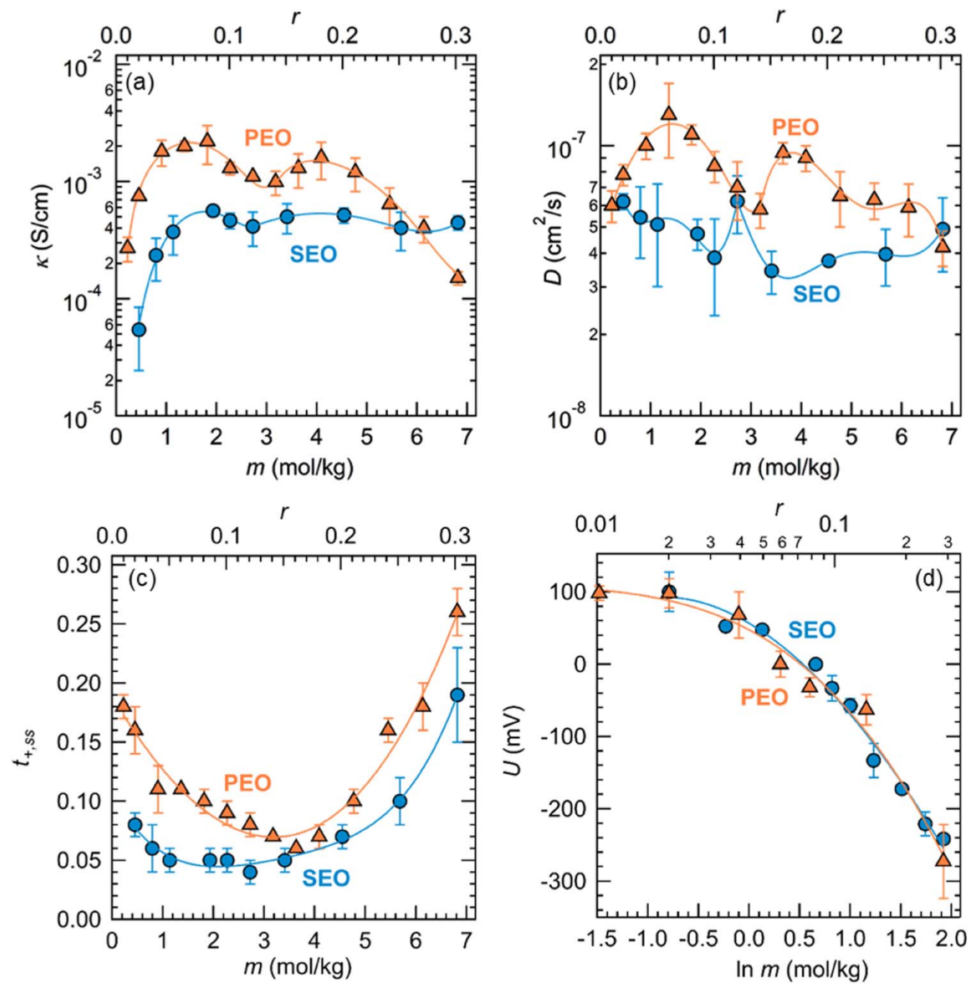

Figure 1. (a) Conductivity, κ, (b) restricted diffusion coefficient, D, (c) the steady-state current transference number, $t_{+,SS}$ as a function of salt concentration, m, and (d) the concentration potential as a function of molality, m, for PEO and SEO electrolytes at 90°C. The solid curves show the best polynomial fits.

where $R_{i,0}$ and $R_{b,0}$ are interfacial and bulk resistances measured by ac impedance spectroscopy prior to polarization.

Restricted-diffusion measurements of SEO electrolytes were performed using the polarization induced by the steady-state current experiment. The applied current was removed, and the cells were allowed to relax for up to 4 h while the open-circuit voltage, U, was measured at time intervals of 1 s. In the simple case where the (t) is a single exponential, the data are fit to the functional form

$$U(t) = k_0 + ae^{-bt}, \quad [9]$$

where a and b are the fit parameters and k_0 is an empirically determined offset voltage. We posit that offset voltage, k_0, arises from small differences in the polymer/lithium interfaces in the symmetric cells. The offset voltage is much smaller than U over most of the experimental window.

$$D = \frac{L^2 b}{\pi^2}, \quad [10]$$

where b is from the fit of Equation 9 and L is the thickness of the electrolyte. The lower limits of the fits are such that $Dt/L^2 > 0.05$.

Concentration cells of SEO electrolytes were prepared using a similar cell configuration as that described in Ref. 20. SEO electrolytes were contained within Garolite-10 spacer. A channel approximately 2.5 cm long and 0.4 cm wide was cut in the Garolite-10 spacer. Half of the channel was filled with reference electrolyte ($m_{ref} = 1.93$ mol/kg), and the other half was filled with electrolytes at various m. Lithium metal electrodes were placed on either end of the channel. Nickel tabs were secured to lithium metal electrodes, and the assembly was vacuum sealed in a laminated aluminum pouch material. Two or three concentration cells were prepared for each salt concentration. The open-circuit voltage, U, was measured for each cell at 90°C using a Biologic VMP3 potentiostat.

The cells were annealed at 90°C for a minimum of two hours prior to commencing the electrochemical measurements.

Results and Discussion

Ionic conductivity, κ, measured using ac impedance, is plotted as a function of salt concentration in Figure 1a. Salt concentration is expressed in terms of molality, m. For convenience, the top x axis in all figures shows salt concentration expressed as r. Figure 1a for PEO and SEO electrolytes indicates that κ has a nonmonotonic dependence on m for both electrolytes, reaching a maximum of 2.21×10^{-3} S/cm at $m = 1.82$ mol/kg and 5.64×10^{-4} S/cm at $m = 1.93$ mol/kg, respectively. The ionic conductivity of PEO electrolytes exhibits two local maxima with the shallow minimum at $m = 3.18$ mol/kg. The second maximum is obtained at $m = 4.09$ mol/kg. In contrast, the conductivity of SEO electrolytes at high salt concentrations ($1.93 \leq m \leq 6.82$ mol/kg) is nearly constant.

Figure 1b shows the salt diffusion coefficient, D, over the same range of salt concentrations for PEO and SEO electrolytes. The PEO data exhibit two shallow maxima at m values where maxima were observed in conductivity. The salt diffusion coefficient in SEO is nearly independent of salt concentration (within experimental error).

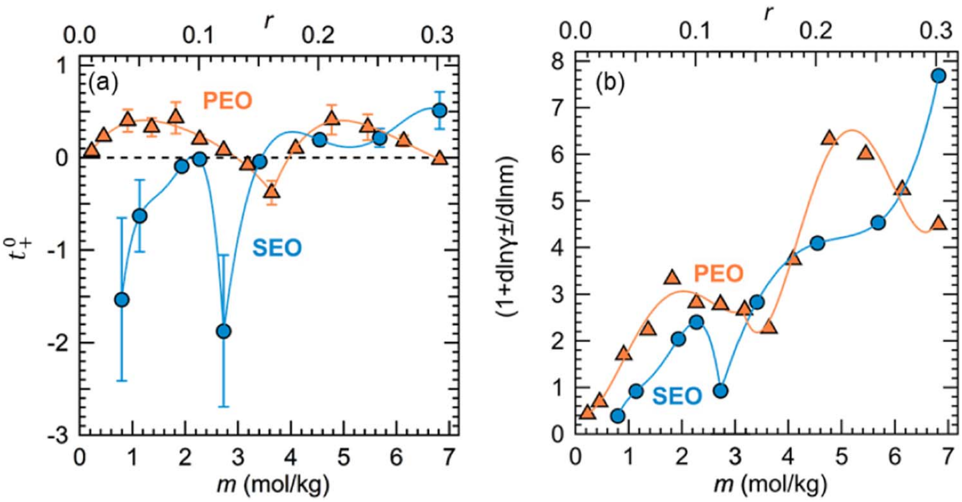

Figure 2. (a) Concentrated solution transference number, t_+^0, and (b) thermodynamic factor, 1+ $d\ln\gamma\pm/d\ln m$, as a function of salt concentration, *m,* for PEO and SEO electrolytes at 90°C. The solid lines are fits through the data.

The approximate transference number, $t_{+,SS}$, based on the assumption of an ideal dilute electrolyte, is plotted as a function of salt concentration, *m*, in Figure 1c. Both PEO and SEO electrolytes exhibit similar trends. In PEO electrolytes, we find that $t_{+,SS}$ reaches a minimum of 0.06 at $m = 3.64$ mol/kg. In SEO electrolytes, we find that $t_{+,SS}$ reaches a minimum of 0.04 at $m = 2.73$ mol/kg. These trends are in good agreement with the literature.[26,18,20]

The open-circuit potential across concentration cells wherein the salt concentration at one electrode was changed while that at the other was held fixed, *U*, was measured. The fixed salt concentrations were $m = 1.36$ mol/kg for PEO electrolytes and $m = 1.93$ mol/kg for SEO electrolytes. The results of these experiments are shown in Figure 1d. The curves in Figure 1d show the best-fit polynomial equations of the form

$$U_{\mathrm{PEO}} = 47.478 - 70.320\,(\ln m) - 33.145\,(\ln m)^2 - 8.052\,(\ln m)^3 \quad [11]$$

$$U_{\mathrm{SEO}} = 56.30 - 82.69\,(\ln m) - 44.81(\ln m)^2 + 1.77\,(\ln m)^3 \quad [12]$$

where *m* has units of mol/kg and *U* is in mV. The trends of *U* vs ln*m* in PEO and SEO are very similar; it is evident that attaching nonconducting polystyrene block to PEO has negligible effect on open-circuit potential.

The cation transference number, t_+^0, is related to *U* by the following equation:[20]

$$t_+^0 = 1 + \left(\frac{1}{t_{+,\mathrm{SS}}} - 1\right)\frac{(z_+\nu_+)FDc\phi_c}{\kappa}\left(\frac{d\ln m}{dU}\right), \quad [13]$$

where z_+ is the charge on the cation and ν_+ is the number of cations in the dissociated salt (z_- and ν_- are defined similarly for the anion), ϕ_c is the volume fraction of the conducting phase, and *F* is Faraday's constant. In our analysis, we approximate the block copolymer to be a three-component system; we ignore interactions between the salt and the nonconducting polystyrene block. We account for the presence of the nonconducting block by inserting the term ϕ_c in Equation 13. Combining measurements of $t_{+,SS}$, κ, *D*, and $d\ln m/dU$ shown in Figure 1, t_+^0 was calculated as a function of salt concentration, *m*. Figure 2a shows the results of these calculations. Both PEO and SEO electrolytes exhibit maxima in the vicinity of $m = 2$ mol/kg. This is followed by a local minimum at $m = 3.41$ mol/kg for PEO and $m = 2.73$ mol/kg for SEO. The SEO minimum is sharper than the PEO minimum. In the case of PEO, t_+^0 is negative in the vicinity of $m = 3.18$ mol/kg. In the case of SEO, negative t_+^0 values are obtained at all concentrations below 3.41 mol/kg. At high concentrations (*m* greater than 4 mol/kg), t_+^0 values of PEO and SEO are similar. Significant differences between t_+^0 and $t_{+,SS}$ are evident at all concentrations, indicating that the assumption of ideality does not apply to PEO/LiTFSI and SEO/LiTFSI electrolytes.

The thermodynamic factor, 1+ $d\ln\gamma_\pm/d\ln m$ is calculated using $dU/d\ln m$ and the anion transference number, t_-^0, according to

$$\left(1 + \frac{d\ln\gamma_\pm}{d\ln m}\right) = -\frac{(z_+\nu_+)}{\nu}\frac{F}{2RTt_-^0}\left(\frac{dU}{d\ln m}\right) \quad [14]$$

where $t_-^0 = 1 - t_+^0$ and $\nu = \nu_+ + \nu_-$. The thermodynamic factors are plotted in Figure 2b for PEO and SEO electrolytes. The thermodynamic factors for both electrolytes are similar, suggesting that the environments of the salt ions in both systems are similar. This is expected in strongly microphase separated block copolymer electrolytes compared to homopolymer electrolytes. It also provides justification for treating SEO/LiTFSI mixtures as a three-component system and for our assumption that the salt interacts only with the PEO domains. Over most of our concentration window, the thermodynamic factor is significantly greater than unity. This is another indication PEO/LiTFSI and SEO/LiTFSI electrolytes are nonideal. (The thermodynamic factor of ideal mixtures is unity).

The data for κ, *D*, $t_{+,SS}$, and $d\ln m/dU$ were fit to polynomial expressions (shown as curves in Figures 1 and 2), and the coefficients obtained from fitting are given in Tables III and IV. The fits were broken up into two regions in PEO and SEO electrolytes for accuracy.

Following the Newman approach,[21] Stefan-Maxwell diffusion coefficients are calculated from the transport parameters given Figures 1 and 2 using the following equations:

$$\mathfrak{D} = \frac{D\,c_0}{c_T\left(1 + \frac{d\ln\gamma_\pm}{d\ln m}\right)}, \quad [15]$$

$$\mathfrak{D}_{+,0} = \frac{\mathfrak{D}}{2\left(1 - t_+^0\right)}, \quad [16]$$

$$\mathfrak{D}_{-,0} = \frac{\mathfrak{D}}{2t_+^0}, \quad [17]$$

$$\mathfrak{D}_{+,-} = \left(\frac{c_T F^2 \phi_c}{\kappa RT} - \frac{2c_0 t_+^0\left(1 - t_+^0\right)}{c_T\mathfrak{D}}\right)^{-1}, \quad [18]$$

$$\mathfrak{D} = \frac{\mathfrak{D}_{+,0}\mathfrak{D}_{-,0}\,(z_+ - z_-)}{z_+\mathfrak{D}_{+,0} - z_-\mathfrak{D}_{-,0}}, \quad [19]$$

Table III. The best-fit polynomial equations of all transport properties in PEO electrolytes.

P_{PEO}	K_0	K_1	K_2	K_3	K_4
$P_{PEO}(m) = K_0 + K_1m + K_2m^2 + K_3m^3 + K_4m^4$ for $m \leq 3.18$					
κ	-3.5503×10^{-4}	2.5863×10^{-3}	3.5520×10^{-4}	-9.3371×10^{-4}	1.9143×10^{-4}
D	4.4177×10^{-8}	6.0464×10^{-8}	4.5163×10^{-8}	-4.7689×10^{-8}	8.7992×10^{-9}
$t_{+,SS}$	0.18907	−0.073386	0.01119	-9.5623×10^{-5}	3.7205×10^{-5}
t_+^{0*}	−0.13847	1.0953	−0.73543	0.1920	−0.021317
$(1 + \frac{d\ln\gamma_\pm}{d\ln m})$	0.4905	−1.058	4.1551	−2.0966	0.3026
$P_{PEO}(m) = K_0 + K_1m + K_2m^2 + K_3m^3 + K_4m^4$ for $m > 3.18$					
P_{PEO}	K_0	K_1	K_2	K_3	K_4
κ	−0.031619	0.024055	-6.2359×10^{-3}	6.8038×10^{-4}	-2.6834×10^{-5}
D	-4.6814×10^{-6}	3.9542×10^{-6}	-1.2003×10^{-6}	1.5822×10^{-7}	-7.6769×10^{-9}
$t_{+,SS}$	0.18907	−0.073386	0.01119	-9.5623×10^{-5}	3.7205×10^{-5}
t_+^{0*}	−28.534	17.881	−4.0355	0.39526	−0.014382
$(1 + \frac{d\ln\gamma_\pm}{d\ln m})$	269.97	−234.53	74.288	−10.052	0.49342

*Note: The fits for t_+^0 were broken up for $m \leq 3.64$ and $m > 3.64$.

Table IV. The best-fit polynomial equations of all transport properties in SEO electrolytes.

P_{SEO}	K_0	K_1	K_2	K_3	K_4
$P_{SEO}(m) = K_0 + K_1m + K_2m^2 + K_3m^3 + K_4m^4$ for $m \leq 2.73$					
κ	1.0034×10^{-4}	-6.4526×10^{-4}	1.5754×10^{-3}	-8.3739×10^{-4}	1.3266×10^{-4}
D	1.3005×10^{-7}	-2.5797×10^{-7}	3.0317×10^{-7}	-1.4755×10^{-7}	2.4828×10^{-8}
$t_{+,SS}$	0.10729	−0.08082	0.036579	-6.9708×10^{-3}	5.2869×10^{-4}
t_+^0	−15.119	35.983	−33.406	13.792	−2.1003
$(1 + \frac{d\ln\gamma_\pm}{d\ln m})$	−1.7283	6.2928	−7.2744	4.2219	−0.83289
$P_{SEO}(m) = K_0 + K_1m + K_2m^2 + K_3m^3 + K_4m^4$ for $m > 2.73$					
P_{SEO}	K_0	K_1	K_2	K_3	K_4
κ	3.9592×10^{-3}	-3.8302×10^{-3}	1.4792×10^{-3}	-2.3846×10^{-4}	1.3614×10^{-5}
D	1.2819×10^{-6}	-1.0616×10^{-6}	3.3096×10^{-7}	-4.4858×10^{-8}	2.2385×10^{-9}
$t_{+,SS}$	0.10729	−0.08082	0.036579	-6.9708×10^{-3}	5.2869×10^{-4}
t_+^0	−62.381	50.597	−15.034	1.9447	−0.092352
$(1 + \frac{d\ln\gamma_\pm}{d\ln m})$	−10.8036	2.479	2.056	−0.64835	0.051621

where $\mathfrak{D}$ is the Stefan-Maxwell diffusion coefficient of the electrolyte based on a thermodynamic driving force, c_0 is the concentration of solvent, $c_T = 2c + c_0$ is the total electrolyte concentration, $\mathfrak{D}_{+,0}$ is the Stefan-Maxwell diffusion coefficient describing the interactions between Li^+ and PEO, and $\mathfrak{D}_{-,0}$ is the Stefan-Maxwell diffusion coefficient describing the interactions between TFSI and PEO, $\mathfrak{D}_{+,-}$ is the Stefan-Maxwell diffusion coefficient describing interactions between Li^+ and $TFSI^-$. For the case of univalent salts,

$$\frac{1}{\mathfrak{D}} = \frac{1}{2}\left(\frac{1}{\mathfrak{D}_{+,0}} + \frac{1}{\mathfrak{D}_{-,0}}\right). \qquad [20]$$

Equations 16–20 place constraints on the values of $\mathfrak{D}_{i,j}$. In particular, if t_+^0 is negative then $\mathfrak{D}_{+,0}$ must be positive and $\mathfrak{D}_{-,0}$ must be negative (see Equations 16 and 17). Returning to the example in the introduction, if $t_+^0 = -1$, then the combination $\mathfrak{D}_{+,0} = +1$ and $\mathfrak{D}_{-,0} = -2$ is consistent with the second law of thermodynamics (the combination $\mathfrak{D}_{+,0} = -1$ and $\mathfrak{D}_{-,0} = +2$ is not). The overall Stefan-Maxwell diffusion coefficient $\mathfrak{D}$ must be positive. This implies that $\mathfrak{D}_{+0}$ must be smaller than the magnitude of $\mathfrak{D}_{-,0}$ when $\mathfrak{D}_{-,0}$ is negative (see Equation 20).

The Stefan-Maxwell diffusion coefficients, $\mathfrak{D}_{+,0}$, for PEO and SEO electrolytes, calculated using Equation 16, are plotted as a function of salt concentration, m, in Figure 3. The data points in Figure 3 present the salt concentrations at which transport coefficients were measured. The curves in Figure 3 were obtained by substituting the polynomial fits for D and the thermodynamic factor into Equation 15 to obtain an expression for $\mathfrak{D}$, and substituting this expression and the polynomial expression for t_+^0 into Equation 16. We see in Figure 3, $\mathfrak{D}_{+,0}$ of PEO and SEO electrolytes are positive and show similar trends. In general, $\mathfrak{D}_{+,0}$ decreases with increasing m. Both sets of data exhibit local maxima at $m = 3.64$ mol/kg (PEO) and $m = 2.73$ mol/kg (SEO). The agreement between PEO and SEO data in Figure 3 indicates that the presence of polystyrene domains in SEO have little effect on the Stefan-Maxwell diffusion coefficients corresponding to cation motion through poly(ethylene oxide) domains.

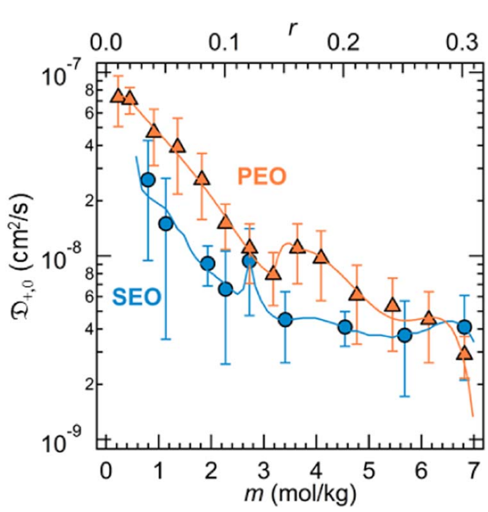

Figure 3. The Stefan-Maxwell diffusion coefficient ($\mathfrak{D}_{+,0}$) for (a) PEO and (b) SEO electrolytes as a function of salt concentration, m, at 90°C. The data points correspond to the measurements in Figure 1 and Figure 2, while the curves are obtained from the polynomial fits given in Tables III and IV.

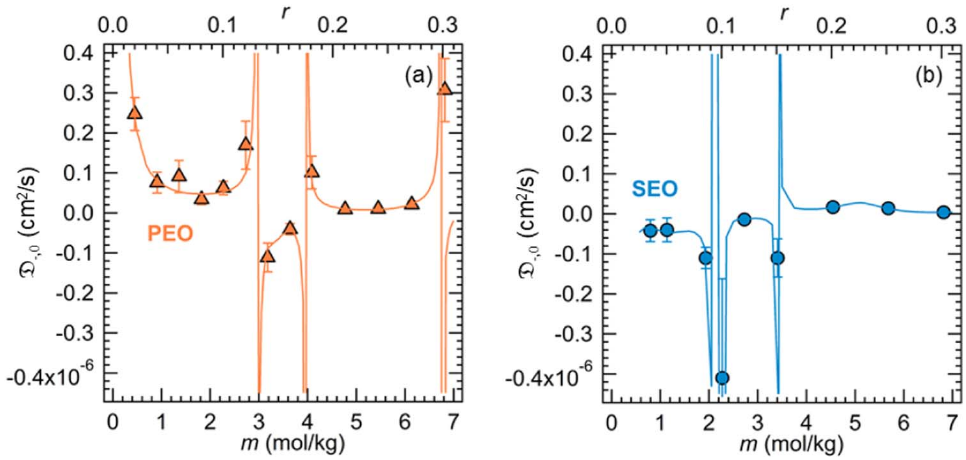

Figure 4. The Stefan-Maxwell diffusion coefficient ($\mathfrak{D}_{-,0}$) for (a) PEO and (b) SEO electrolytes as functions of salt concentration, m, at 90°C. The data points correspond to the measurements in Figure 1 and Figure 2, while the curves are obtained from the polynomial fits given in Tables II and IV.

The Stefan-Maxwell diffusion coefficient, $\mathfrak{D}_{-,0}$, for PEO electrolytes, calculated using Equation 17, are plotted as a function of salt concentration, m, in Figure 4a. As was the case in Figure 3, the data points present the salt concentrations at which transport coefficients were measured, while the curves were obtained from the polynomial fits (Equation 17). The plot of $\mathfrak{D}_{-,0}$ for PEO versus salt concentration is much more complex than the plot of $\mathfrak{D}_{+,0}$ versus salt concentration. The $\mathfrak{D}_{-,0}$ versus m plot for PEO contains three minima at $m = 3.00$, 3.95, and 6.75 mol/kg (PEO). $\mathfrak{D}_{-,0}$ is positive at salt concentrations $0.23 \leq m \leq 2.73$ mol/kg and $4.09 \leq m \leq 6.14$ mol/kg and negative values at $3.18 \leq m \leq 3.64$ mol/kg. $\mathfrak{D}_{-,0}$ is also negative at the highest salt concentration studied, $m = 6.82$ mol/kg.

Note that $\mathfrak{D}_{-,0}$ approaches a singularity when t_+^0 approaches 0 (see Equation 17). This occurs at $m = 0.23$, 2.73, 3.18, 3.64, and 6.82 mol/kg in Figure 4a. The singularities are poles: $\mathfrak{D}_{-,0}$ approaches $+\infty$ as t_+^0 approaches 0^+, and $\mathfrak{D}_{-,0}$ approaches $-\infty$ as t_+^0 approaches 0^-. For example, $\mathfrak{D}_{-,0}$ swings from $+\infty$ to $-\infty$ as salt concentration changes from $m = (2.967 - \delta)$ to $(2.967 + \delta)$ mol/kg, where δ is infinitesimally small. Such swings are impossible to capture in experiments where m is changed in finite steps.

Figure 4b shows a plot of $\mathfrak{D}_{-,0}$ versus m for SEO electrolytes. This plot is entirely analogous to Figure 4a. In SEO electrolytes, $\mathfrak{D}_{-,0}$ exhibits singularities at $m = 1.93$, 2.27, and 3.41 mol/kg that are qualitatively similar to those seen in PEO electrolytes.

The dependence of $\mathfrak{D}_{+,-}$ on m for PEO and SEO electrolytes is shown in Figures 5a and 5b. These data also contain singularities when

$$\frac{c_T F^2 \phi_c}{\kappa RT} = \frac{2c_0 t_+^0 \left(1 - t_+^0\right)}{c_T \mathfrak{D}}, \quad [21]$$

as required by Equation 18. The poles in Figure 5 appear at salt concentrations where Equation 21 is satisfied.

It is also important to note that in the vicinity of singularities when a particular $\mathfrak{D}_{ij}$ is large, it means that transport is governed by the other relevant Stefan-Maxwell diffusion coefficients; $\mathfrak{D}_{ij}$ appear in the denominator of the right side of Equation 1. For example, in the vicinity of $m = 2.73$ mol/kg where $\mathfrak{D}_{-,0}$ approaches either $+\infty$ or $-\infty$, the flux of the anion is entirely determined by the magnitude and sign of $\mathfrak{D}_{+,-}$.

In Figure 6a, we plot $1/\mathfrak{D}_{-,0}$ versus m for PEO and SEO electrolytes. In both cases we see two maxima separated by a minimum in the vicinity of $m = 3$ mol/kg. The low salt concentration maxima are shallow, relative to the high salt concentration maxima in both systems. Except for the highest salt concentration studied, there is reasonable agreement between the two electrolytes. In Figure 6b, we plot $1/\mathfrak{D}_{+,-}$ versus m for PEO and SEO electrolytes. In both cases, we see a maximum in the middle of our salt concentration window. In

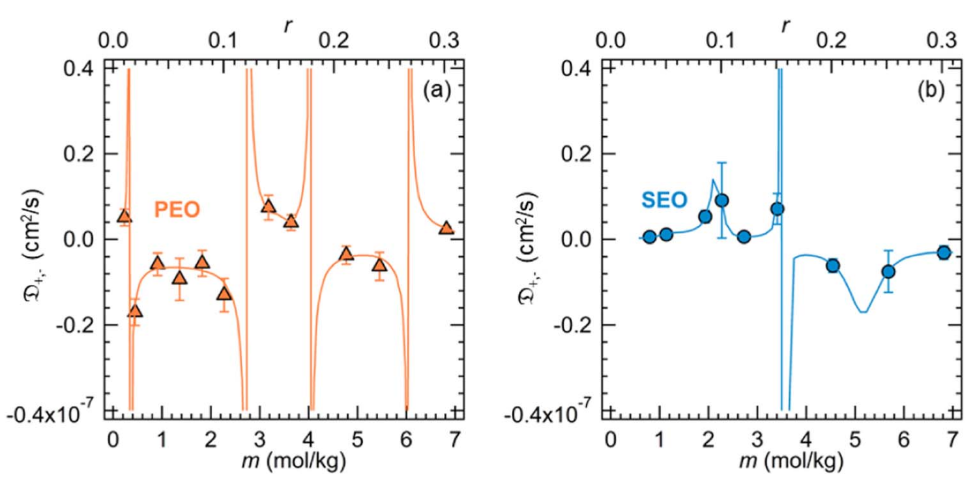

Figure 5. The Stefan-Maxwell diffusion coefficient ($\mathfrak{D}_{+,-}$) for (a) PEO and (b) SEO electrolytes as functions of salt concentration, m, at 90°C. The data points correspond to the measurements in Figure 1 and Figure 2, while the curves are obtained from the polynomial fits given in Tables III and IV. In some cases, error bars are smaller than the size of the data markers.

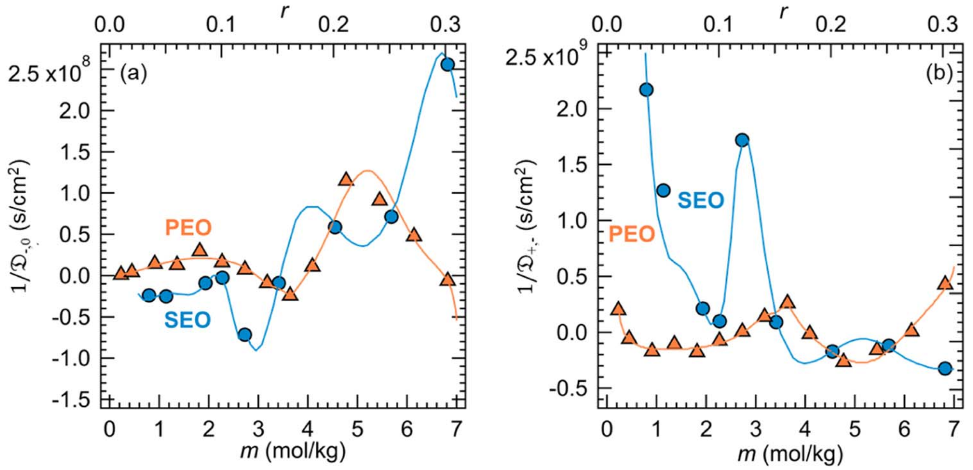

Figure 6. Stefan-Maxwell diffusion coefficients (a) $1/\mathfrak{D}_{-,0}$ and (b) $1/\mathfrak{D}_{+,-}$ for PEO and SEO electrolytes as functions of salt concentration, m, at 90°C. The data points correspond to the measurements in Figures 1 and Figure 2, while the curves are obtained from the polynomial fits given in Tables III and IV. Uncertainties in $\mathfrak{D}_{-,0}$ and $\mathfrak{D}_{+,-}$ not shown explicitly for clarity. They are given in Figures 4 and 5.

cases where poles are obtained in $\mathfrak{D}_{ij}$ versus salt concentration plots, it is preferable to change the abscissa to $1/\mathfrak{D}_{ij}$.

The physical implications of negative transference numbers and Stefan-Maxwell diffusion coefficients is that LiTFSI does not dissociate into Li^+ and $TFSI^-$ ions that migrate independently under the influence of the applied electric field. When t_+^0 is negative, it implies that when a field is applied to an electrolyte with uniform composition, both the Li^+ and $TFSI^-$ are driven to the positive electrode (we assume that the motion of the polymer chains induced by the electric field can be ignored). This, in turn, may imply the presence of a multitude of charged clusters in the electrolyte. If, for example, there are three species in solution, Li^+, $TFSI^-$, and $[Li(TFSI)_2]^-$, then a negative transference number would arise if the dominant mobile species were $TFSI^-$, and $[Li(TFSI)_2]^-$. The Stefan-Maxwell diffusion coefficients $\mathfrak{D}_{ij}$ that we have obtained represent the frictional interactions between all manifestations of a particular species. A powerful property of the Stefan-Maxwell formalism is that it applies regardless of the nature of the associations in solution. A limitation of the Stefan-Maxwell formalism is that it provides limited information on the nature of the associations that underlie the measured diffusion coefficients. Negative transference numbers in our electrolytes could arise due to the presence of $[Li(TFSI)_2]^-$ or $[Li_2(TFSI)_3]^-$ or some other negatively charged cluster. Such information must be provided by other independent experiments (e.g. spectroscopic experiments such as Raman or NMR).

Conclusions

We present complete electrochemical transport characterization of a microphase-separated SEO block copolymer electrolyte by reporting κ, D, and t_+^0 as well as the thermodynamic factor as functions of salt concentration. We compare the properties of the block copolymer electrolyte with those of PEO homopolymer electrolytes. Negative values of t_+^0 are observed in many cases. The nature of frictional interactions between the components of the electrolytes (ions and polymer chains) is elucidated by determining the Stefan-Maxwell diffusion coefficients ($\mathfrak{D}_{+,0}$, $\mathfrak{D}_{-,0}$, and $\mathfrak{D}_{+,-}$) from the electrochemical characterization data. It may be possible to examine these interactions independently using techniques such as electrophoretic NMR.[14–17,23] The complete electrochemical characterization data for SEO and PEO electrolytes presented here is necessary for modeling charge-discharge characteristics of cells that contain these electrolytes.

Acknowledgments

This work was intellectually led by the Joint Center for Energy Storage Research (JCESR), an Energy Innovation Hub funded by the U.S. Department of Energy (DOE), Office of Science, Basic Energy Sciences (BES), under Contract No. DEAC02-06CH11357.

List of Symbols

a, b	fit parameters in the Equation 9
c	salt concentration (mol/L)
c_i	concentration of species i (mol/L)
c_j	concentration of species i (mol/L)
c_0	concentration of the solvent (mol/L)
c_T	total electrolyte concentration (mol/L)
D	salt diffusion coefficient (cm^2/s)
$\mathfrak{D}$	diffusion coefficient of electrolyte, based on a thermodynamic driving force (cm^2/s)
$\mathfrak{D}_{ij}$	diffusion coefficient for interaction of species i and j (cm^2/s)
$\mathfrak{D}_{+,0}$	Stefan-Maxwell diffusion coefficient describing the interactions between Li and PEO (cm^2/s)
$\mathfrak{D}_{-,0}$	Stefan-Maxwell diffusion coefficient describing the interactions between TFSI and PEO (cm^2/s)
$\mathfrak{D}_{+,-}$	Stefan-Maxwell diffusion coefficient describing the interactions between Li and TFSI (cm^2/s)
F	Faraday's constant (96485 C/mol)
i_0	initial current (mA/cm^2)
i_{ss}	steady-state current (mA/cm^2)
k_0	offset voltage (mV)
L	thickness of the electrolyte (cm)
LiTFSI	lithium bis(trifluoromethanesulfonyl) imide
m	molality (mol/kg)
m_{ref}	concentration of reference electrolyte used in concentration cells (mol/kg)
M_{EO}	molar mass of the ethylene oxide repeat unit (44.05 g/mol)
M_{LiTFSI}	molar mass of LiTFSI (287.09 g/mol)
PEO	poly(ethylene oxide)
r	moles of Li^+ per mole of ethylene oxide
R	gas constant (8.314 J/(mol K))
$R_{b,0}$	bulk resistance (Ω cm^2)
$R_{i,0}$	initial interfacial resistance (Ω cm^2)
$R_{i,SS}$	steady-state interfacial resistance (Ω cm^2)
S	cross-sectional area of the spacer (cm^2)
SEO	polystyrene-*b*-poly(ethylene oxide)
t	time (h)
t_+^0	transference number obtained using Balsara and Newman method

$t_{+,SS}$	transference number obtained using stead-state current method
T	temperature (K)
U	open-circuit voltage (mV)
$\mathbf{v}_i$, $\mathbf{v}_j$	velocity of species i and j (cm/s)
$\mathbf{v}_0$	velocity of the solvent (cm/s)
$\mathbf{v}_+$, $\mathbf{v}_-$	velocity of the cation and the anion (cm/s)

Greek

ΔV	applied potential (mV)
z_+, z_-	charge number on the cation and anion
$\gamma_\pm$	mean molal activity coefficient of the salt
κ	ionic conductivity (S/cm)
μ_i	electrochemical potential of species i (J/mol)
ν_+, ν_-	number of cations and anions in the dissociated salt
ρ	density of the electrolyte (g/L)
ϕ_c	volume fraction of the conducting phase
$1+d\ln\gamma_\pm/d\ln m$	thermodynamic factor

ORCID

Irune Villaluenga https://orcid.org/0000-0002-1299-2479
Ksenia Timachova https://orcid.org/0000-0001-8200-3552
Venkat Srinivasan https://orcid.org/0000-0002-1248-5952
Nitash P. Balsara https://orcid.org/0000-0002-0106-5565

References

1. P. G. Bruce, B. Scrosati, and J. M. Tarascon, *Angew. Chem. Int. Ed.*, **47**, 2930 (2008).
2. M. B. Armand, *Annu. Rev. Mater. Sci.*, **16**, 245 (1986).
3. D. T. H. Jr and N. P. Balsara, *Annu. Rev. Mater. Res.*, **43**, 503 (2013).
4. M. Singh, O. Odusanya, G. M. Wilmes, H. B. Eitouni, E. D. Gomez, A. J. Patel, V. L. Chen, M. J. Park, P. Fragouli, H. Iatrou, N. Hadjichristidis, D. Cookson, and N. P. Balsara, *Macromolecules*, **40**, 4578 (2007).
5. P. P. Soo, B. Huang, Y. I. Jang, Y. M. Chiang, D. R. Sadoway, and A. M. Mayes, *J. Electrochem. Soc.*, **146**, 32 (1999).
6. S. A. Mullin, G. M. Stone, A. Panday, and N. P. Balsara, *J. Electrochem. Soc.*, **158**, A619 (2011).
7. S. Stewart and J. Newman, *J. Electrochem. Soc.*,**155**, A458 (2008).
8. H. Hafezi and J. Newman, *J. Electrochem. Soc.*, **147**, 3036 (2000).
9. G. Orädd, L. Edman, and A. Ferry, *Solid State Ionics*, **152**, 131 (2002).
10. D. Devaux, R. Bouchet, D. Glé, and R. Denoyel, *Solid State Ionics*, **227**, 119 (2012).
11. A. A. Teran, M. H. Tang, S. A. Mullin, and N. P. Balsara, *Solid State Ionics*, **203**, 18 (2011).
12. M. Watanabe, S. Nagano, K. Sanui, and N. Ogata, *Solid State Ionics*, **28**, 911 (1988).
13. J. Evans, C. A. Vincent, and P. G. Bruce, *Polymer*, **28**, 2324 (1987).
14. S. Bhattacharja, S. W. Smoot, and D. H. Whitmore, *Solid State Ionics*, **18**, 306 (1986).
15. Z. Zhang and L. A. Madsen, *J. Chem. Phys.*, **140**, 084204 (2014).
16. J. Hou, Z. Zhang, and L. A. Madsen, *J. Phys.Chem. B*, **115**, 4576 (2011).
17. H. Dai and T. A. Zawodzinski, *J. Electrochem. Soc.*, **143**, L107 (1996).
18. D. M. Pesko, K. Timachova, R. Bhattacharya, M. C. Smith, I. Villaluenga, J. Newman, and N. P. Balsara, *J. Electrochem. Soc.*, **164**, E3569 (2017).
19. N. P. Balsara and J. Newman, *J. Electrochem. Soc.*, **162**, A2720 (2015).
20. K. Timachova, I. Villaluenga, L. Cirrincione, M. Gobet, R. Bhattacharya, X. Jiang, J. Newman, L. A. Madsen, S. G. Greenbaum, and N. P. Balsara, *J. Phys. Chem. B*, **122**, 1537 (2018).
21. M. Doyle and J. Newman, *J. Electrochem. Soc.*, **142**, 3465 (1995).
22. J. Newman and K. E. Thomas-Alyea, *Electrochemical Systems*, John Wiley & Sons, New Jersey (2004).
23. M. Gouverneur, F. Schmidta, and M. Schönhoff, *Phys. Chem. Chem. Phys.*, **20**, 7470 (2018).
24. R. Yuan, A. A. Teran, I. Gurevitch, S. A. Mullin, N. S. Wanakule, and N. P. Balsara, *Macromolecules*, **46**, 914 (2013).
25. S. N. Patel, A. E. Javier, G. M. Stone, S. A. Mullin, and N. P. Balsara, *ACS Nano*, **6**, 1589 (2012).
26. K. Pożyczka, M. Marzantowicz, J. R. Dygas, and F. Krok, *Electrochimica Acta*, **227**, 127 (2017).